ENDOLUMINAL LOOP RADIOFREQUENCY COILS FOR GASTROINTESTINAL WALL IMAGING

M. Armenean[1,2], O. Beuf[2], F. Pilleul[3], H. Saint-Jalmes[2], Member IEEE

[1]Dept. of Physics, Babes-Bolyai University, Cluj-Napoca, Romania
[2] Laboratoire de RMN, UMR CNRS 5012, Université Claude Bernard Lyon 1 – ESCPE Lyon, France
[3]Service de Radiologie Digestive, Hôpital Edouard Herriot, Lyon, France

Abstract-**In this paper, we describe the optimization of endoluminal planar coils for high-resolution Magnetic Resonance Imaging (MRI) of gastrointestinal walls. Based on simulations, single-loop RF coils were designed. Experimental verifications were performed on a 1.5 T clinical scanner. Developed prototypes provided a dramatic increase in signal-to-noise ratio at the region of interest.**
***Keywords* - RF coils, endoluminal, MRI, gastrointestinal wall**

I. INTRODUCTION

Due to recent technical advances, MRI is now widely used in clinical routine for diagnosis and staging of digestive diseases [1]. Indeed, dedicated external radiofrequency (RF) coils placed close to the area of interest have dramatically enhanced image quality. However, due to the importance of magnetic losses in the human body, detailed information about the gastrointestinal wall layers are still not available. Based on recent work in intravascular application of receiver coils for high-resolution MRI of vascular walls [2, 3], prototype endoluminal MR receiver coils were designed to be inserted in the digestive system.

Based on the constraints and requirements of the endoluminal approach for MRI, the outer diameter of the coils was fixed to 5 mm (Fig. 1).

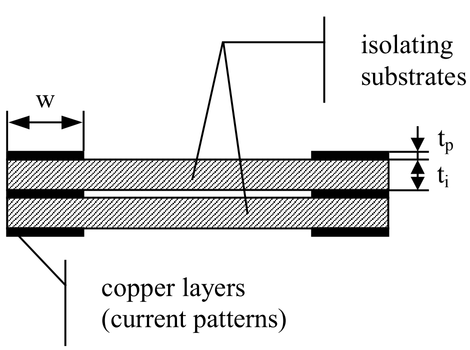

Fig. 1. General cross section of the coils optimized in this study.

II. METHODOLOGY

For optimizing not only the quality factor (Q) but also the signal-to-noise ratio (SNR), we simulated the electromagnetic parameters (the electrical resistance R_{noise}, the inductance L and the RF field B_1) of planar rectangular RF coils using ANSOFT Maxwell 2D/3D software (Ansoft Corp., Pittsburgh, USA) and Magnetic@ (MagneticaSoft, Nice, France). The Maxwell 2D/3D software is based on advanced finite element technology and uses electromagnetic AC and DC field simulation to predict product performance with physical and geometric input. Magnetic@, works under Mathematica software (Wolfram Research, Inc., USA) and provides high accurate computations of static magnetic field [4]. This software offers the choice of two modes of calculation: a method derived from the vector potential which is applicable to all space including the winding and the magnetic materials and a method using spherical harmonics which is restricted to the space without magnetic field generator. The simulations were been performed using magnetostatic approximation in order to calculate the B_1 field and sinusoidal excitation of the RF coil in order to calculate the resistance R_{noise} of the coils and the magnetic losses.

The SNR of a NMR experiment is defined as the peak signal divided by the root mean square (rms) noise [5]:

$$\mathrm{SNR} = \frac{\text{peak signal}}{\text{RMS noise}} = \frac{\frac{B_1}{i}\omega_0 M_0 V_S}{\sqrt{4kTR_{noise}\Delta f}} \tag{1}$$

with:

$$M_0 = \frac{N\gamma^2 \hbar I(I+1)B_0}{3kT} \tag{2}$$

where B_1/i is the magnetic field per current unit (*coil sensitivity*), ω_0 the nuclear precession pulsation, M_0 the nuclear magnetization, V_S the sample volume, k the Boltzmann's constant, T the sample temperature, N the spin density, γ the gyromagnetic ratio, I the spin quantum number, $\hbar$ the Planck's constant divided by 2π, B_0 the static magnetic field and Δf is the spectral bandwidth. R_{noise} is the total resistance of the coil, which includes the magnetic losses. According to (1), the performances of the RF receiver coils are driven by the ratio $B_1 / i\sqrt{R_{noise}}$, which have to be optimized.

Invoking the reciprocity principle [6] and assuming the static field B_0 aligned along the z direction, the received RF field B_1 at a given point is defined by:

$$B_1 = \sqrt{B_x^2 + B_y^2} \tag{3}$$

Report Documentation Page

Report Date	Report Type	Dates Covered (from... to)
25 Oct 2001	N/A	-

Title and Subtitle Endoluminal Loop Radiofrequency Coils for Gastrointestinal Wall Imaging	**Contract Number**
	Grant Number
	Program Element Number
Author(s)	**Project Number**
	Task Number
	Work Unit Number
Performing Organization Name(s) and Address(es) Dept. of Physics, Babes-Bolyai University Cluj-Napoca, Romania	**Performing Organization Report Number**
Sponsoring/Monitoring Agency Name(s) and Address(es) US Army Research, Development & Standardization Group (UK) PSC 802 Box 15 FPO AE 09499-1500	**Sponsor/Monitor's Acronym(s)**
	Sponsor/Monitor's Report Number(s)

Distribution/Availability Statement
Approved for public release, distribution unlimited

Supplementary Notes
Papers from 23rd Annual International Conference of the IEEE Engineering in Medicine and Biology Society, October 25-28, 2001, held in Istanbul, Turkey. See also ADM001351 for entire conference on cd-rom., The original document contains color images.

Abstract

Subject Terms

Report Classification unclassified	**Classification of this page** unclassified
Classification of Abstract unclassified	**Limitation of Abstract** UU

Number of Pages
4

where B_x and B_y are the field components orthogonal to B_0.

The origins of noise in NMR are multiple. We have considered the electrical resistance of the isolated coil (in vacuum) and the magnetic losses in the sample as noise sources.

The total resistance of the coil was defined by:

$$R_{noise} = R' + R'' \tag{4}$$

where R' is the electrical resistance of the isolated coil (in vacuum) and R'' is the equivalent electrical resistance due to the magnetic losses in the sample (human body in our case).

The electrical resistance of the isolated coil R' is due to the ohmic losses, the skin effect and the proximity effect in the coil wires. The current is concentrated towards the outer edge of the conductor (skin effect) with the current density decreasing exponentially from the wire surface to the center.

The magnetic field lines from a given turn of coil induce eddy currents in adjacent turns (proximity effect), further distorting the current distribution and increasing the resistance of coil [7, 8].

The computation of the electrical resistance R' for our coils is complicated by the fact that in the case of a wire with rectangular sections, standard calculations rules are no more relevant and the help of an electromagnetic simulation software is mandatory in order to obtain accurate results. For the wires with rectangular section, the current is not uniformly distributed at the surface like in the case of wires with circular section. This effect is more accentuated when the ratio between the sides of rectangular section increases. The distribution of the current density in the cross section of an isolated rectangular wire (0.8 mm width and 70 µm thickness) is shown in Fig. 2.

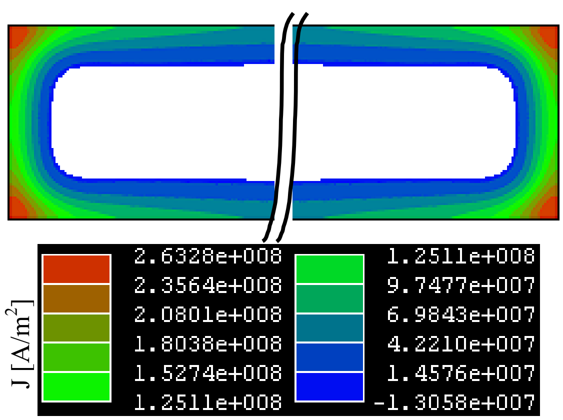

Fig. 2. The distribution of the current density in the cross section of an isolated rectangular infinite long wire for a current I = 1 A.

The RF field produced by the coil induces eddy currents in the sample and this leads to an increase of R_{noise} (R'' increase). At the dimensions of our coils, for a frequency of 63.7 MHz, the noise originating from the sample is comparable with the noise produced by the coil wires.

The noise increases with RF frequency and with the volume of body exposed at the RF field.

In our simulations we varied the number of turns (n = 1, 2 or 3), the number of layers (1, 2 or 3), the thickness of copper layers (t_p = 35 or 70 µm), the thickness of isolating substrate (t_i = 0.8 and 1.6 mm), the coil length (l = 20, 30, 40 or 50 mm) and the width of current patterns (w = 0.6, 0.8 or 2 mm).

The SNR simulations were computed at the frequency of 63.7 MHz, corresponding to the proton resonance frequency at 1.5 T, a sample temperature T = 37 °C (temperature of human body) and various receive spectral bandwidths Δf.

Based on described simulations, two single loop of 20 mm and 40 mm length coil prototypes were built using IC (printed circuit) technology (Fig. 3). Conventional tuning-matching circuits were used to optimize the NMR signal transmission through the coaxial cable. For safety issues and to enable accurate and automatic prescan, an active circuit for transmission-reception decoupling was included. The coils were tuned to a frequency of 63.7 MHz and matched at 50 Ω for this frequency.

The electromagnetic characterization of the coils (R, L and Q) was performed using a network analyzer 4195A (Hewlett Packard).

SNR performance and signal homogeneity tests were performed with the coils inserted in a phantom. The phantom consisted of 6 mm inner diameter tube with 7 mm outer diameter places in a plastic container filled with a 0.9% NaCl solution. This was done to approximate the loading conditions of a coil inserted in a patient. The cylinder was oriented with its axis parallel to B_0. MR images were obtained on a 1.5 T MR Symphony system (Siemens, Erlangen, Germany) using a fast gradient-echo sequence. Imaging parameters were: TR/TE 500/18 ms; 30° flip angle; FOV = 60 mm, 2 mm slice thickness; 128 x 256 matrix; 78 Hz/pixel bandwidth and 66 sec imaging time.

Prior to evaluation of coil performances, decoupling efficiency was ensured by checking the absence of signal highlights in the vicinity of the endoluminal coil while using the body coil of the MR system in transmit-receive mode.

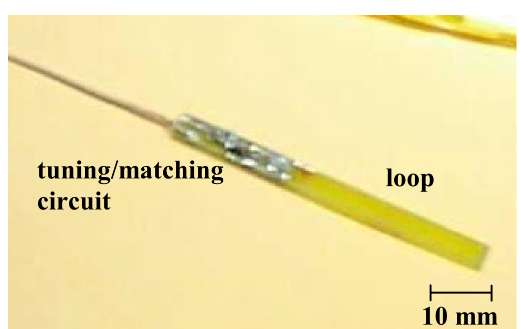

Fig. 3. Photograph of a 40 mm single-loop, single-layer coil prototype.

III. RESULTS

In order to calculate the electrical resistance of the coils, we have simulated infinite long current patterns (copper) in vacuum. This way we obtained the electrical resistance of the current patterns per unit length. The electrical resistance of the coil is obtained multiplying the resistance of the current patterns per unit length with the length of current pattern of the coil.

The distribution of the simulated magnetic losses per unit of coil length for a coil with $n = 2$, $w = 0.8$ mm, $t_p = 70$ µm, $t_i = 1.6$ mm and a current $I = 1$ A in the cross section of the sample (0.9% NaCl solution with the electrical conductivity $\sigma = 1$ S/m) is given in Fig. 4.

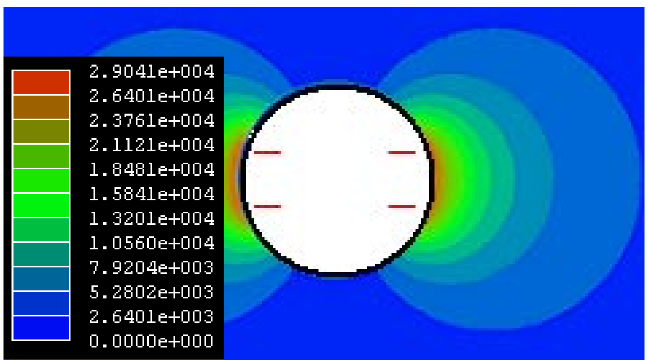

Fig. 4. The distribution of the simulated magnetic losses per unit of coil length in W/m for I = 1 A.

Because the resistance R' of the current patterns decreases by 14 % if the thickness of copper layers t_p increases from 35 µm to 70 µm, $t_p = 70$ µm was chosen for the following simulations.

To start we optimized the width (w) of the current patterns. If w increases from 0.6 mm to 0.8 mm the electrical resistance R' decreases by approximately 26 % and the RF field B_1 remains about the same. This leads to an increase of the $B_1 / i\sqrt{R_{noise}}$ ratio. For a width of current pattern $w = 2$ mm, R' further decreases by approximately 69 % but the diminution of the RF field B_1 is more stronger and the $B_1 / i\sqrt{R_{noise}}$ ratio decreases. Then further simulations are made with $w = 0.8$ mm and $t_p = 70$ µm.

For the next step we have evaluated the influence of the coil length in the $B_1 / i\sqrt{R_{noise}}$ ratio. The results for coils with $w = 0.8$ mm, $t_p = 70$ µm, $n = 1$ turn and different lengths (l) are shown in Fig. 5 at a distance of $x = 3$ mm, 13 mm and 23 mm from coil.

For a current pattern with two layers the electrical resistance R' decreases by approximately 70 % for a insulator thickness $t_i = 0.8$ mm and by 85 % for $t_i = 1.6$ mm. When we have a current pattern with three layers and $t_i = 0.8$ mm the electrical resistance R decreases by approximately 133 %. So, the multi-layer current patterns provides a decreasing of the electrical resistance R of the coil preserving the RF field B_1 and thus increasing the SNR.

In the case of a coil with $n = 1$, $w = 0.8$ mm, $t_p = 70$ µm and $l = 40$ mm the simulated total resistance R_{noise} (including the magnetic losses) is 0.207 Ω. For the same width of current pattern, thickness of copper layer and coil length, if $n = 2$ and $t_i = 1.6$ mm then the total resistance rise to 0.530 Ω. In the same conditions, if $n = 3$ and $t_i = 0.8$ mm, $R_{noise} = 1.023$ Ω. The variations of $B_1 / i\sqrt{R_{noise}}$ ratio for different turns number (assuming: $w = 0.8$ mm, $t_p = 70$ µm, $t_i = 1.6$ mm for the coil with $n = 2$ and 0.8 mm for $n = 3$) are given in Fig. 6.

The measured loaded quality factor Q were 44 and 50 for 20 mm and 40 mm length coils respectively.

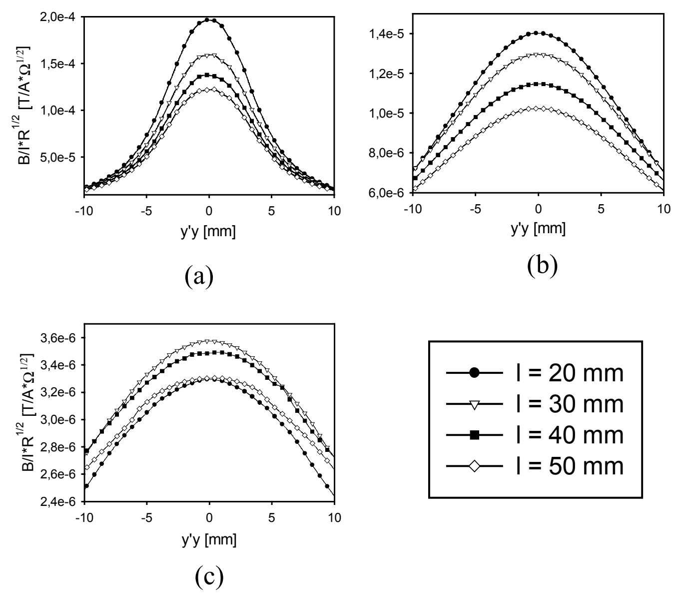

Fig. 5. The coil sensitivity for different coil lengths (l) at a distance of: (a) x = 3 mm, (b) x = 13mm, (c) x = 23 mm from the center of the coil.

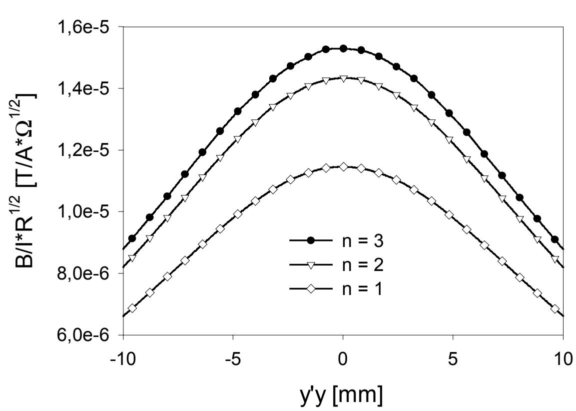

Fig. 6. The coil sensitivity for different turn numbers at a distance x = 13 mm.

Representative phantom images are shown in Fig. 7. The phantom sensitivity patterns fall off rapidly with distance from the coil. In the immediate vicinity of the coil, the "shortest" coil (l = 20 mm) was found more sensitive with higher SNR whereas the "longest" coil (l = 40 mm) results in greater penetration depth. This behavior is in good agreement with computed simulations (Fig. 5), however the distance at which coil sensitivities are inverting is smaller than expected from the simulations. From SNR measurements on concentric circles, the inversion distance was determined at 10 mm from the center of the coil.

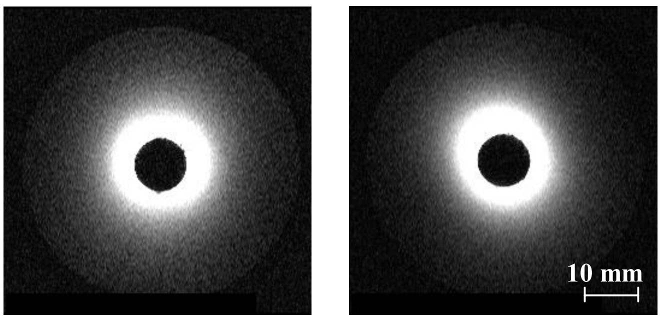

a b

Fig. 7. Comparison of signal characteristics with the receiver single-loop coils inserted in a glass tube embedded in a saline solution. Axial MR images obtained with a) 40 mm length b) 20 mm length coils.

SNR measured in the vicinity of both endoluminal coils were at least 10 times higher than SNR measured with the regular 4-elements phased-array body coil used for digestive clinical exams. The equilibrium in SNR between body array coil and endoluminal coils is obtained at about 20 mm from the center of the region of interest.

IV. Discussion

The proper set-up of the decoupling circuit is a critical factor for homogeneous signal distribution and consistent image quality.

The signal behavior was found in good agreement with computed simulations. The internal coils provide very high sensitivity local to the coil but the sensitivity deteriorates rapidly away from the coil. There is however quantitative differences for tested coils regarding the distance at which sensitivities are inverting. This discrepancy may be due to Q value differences between calculated and measured values. Simulated Q values were 89 and 92 for 20 mm and 40 mm length coils respectively as compared to 44 and 50 for measured Q values. Variations in Q values may be due to electrical resistance variations (ranging from 0.1 to 0.2 Ω) caused by surface printed circuit and solder imperfections. Correcting for SNR by taking into account Q differences, the inversion distance from the center of the coil was calculated at 14 mm. This matches approximately simulated values as shown in Fig. 5.

In any cases, experimental measurements shown that developed endoluminal coils performed better than external coils in term of SNR in a 20 mm radius region centered on the local coils.

V. Conclusion

Endoluminal loop RF coils have been developed for gastrointestinal wall imaging. Performed simulations are in good agreement with experimental results. The internal coils provide a dramatic increase in SNR local to the coil compared to usual external coils. Such coils may provide detailed information about the gastrointestinal wall layers. Further developments will study feasibility and benefits of quadrature detection coils.

Acknowledgment

The authors thank Boualem Azazi for technical assistance in building the coils and Siemens France for providing information and connectors to interface the coils with the MR system.

References

[1] H. E. Adamek, H. Breer, T. Karschkes, J. Albert and J. F. Riemann, "Magnetic resonance imaging in gastroenterology: time to say good-bye to all that endoscopy?", *Endoscopy*, 32, pp. 406-410 (2000).

[2] H. H. Quick, M. E. Ladd, G. G. Zimmermann-Paul, P. Erhart, E. Hofmann, G. K. von Schulthess and J. F. Debatin, "Single-loop coil concepts for intravascular Magnetic Resonance Imaging", *Magn. Reson. Med*, 41, pp. 751-758 (1999).

[3] H. H. Quick, M. E. Ladd, P. R. Hilfiker, G. G. Paul, S-W. Ha and J. F. Debatin, "Autoperfused ballon catheter for intravascular MR Imaging", *JMRI*, 9, pp. 428-434 (1999).

[4] L. Donadieu, H.Saint-Jalmes 44th Annual Conference on Magnetism & Magnetic Materials, Nov. 15-18, 1999, San Jose, California (USA).

[5] D. I. Hoult and R. E. Richards, "The signal-to-noise ratio of the nuclear magnetic resonance experiment", *J. Magn. Reson.*, 24, pp. 71-85, 1976.

[6] G. C. Hurst, J. Hua, J. L. Duerk and A. M. Cohen, "Intravascular (catheter) NMR receiver probe: preliminary design analysis and applications to canine iliofemoral imaging", *Magn. Reson. Med*, 24, pp. 343-357, 1992.

[7] A. G. Webb, "Radiofrequency microcoils in magnetic resonance", *Progress in NMR spectroscopy*, 31, pp. 1-42, 1997.

[8] T. L. Peck, R. L. Magin and P. C. Lauterbur, "Design and analysis of microcoils for NMR microscopy", *J. Magn. Reson.*, Series B 108, pp. 114-124, 1995.